

# Detecting Einstein-Podolsky-Rosen steering and bipartite entanglement in split Dicke states

Giuseppe Vitagliano,<sup>1,2</sup> Matteo Fadel,<sup>3</sup> Iagoba Apellaniz,<sup>4,2</sup>  
Matthias Kleinmann,<sup>5,2</sup> Bernd Lücke,<sup>6</sup> Carsten Klempt,<sup>6</sup> and Géza Tóth<sup>2,7,8,9</sup>

<sup>1</sup>*Institute for Quantum Optics and Quantum Information (IQOQI),  
Austrian Academy of Sciences, A-1090 Vienna, Austria*

<sup>2</sup>*Theoretical Physics, University of the Basque Country UPV/EHU, E-48080 Bilbao, Spain*

<sup>3</sup>*Department of Physics, University of Basel, CH-4056 Basel, Switzerland*

<sup>4</sup>*Mechanical and Industrial Manufacturing Department,  
Mondragon Unibertsitatea, 20500 Mondragón, Spain, E-20500, Spain*

<sup>5</sup>*Naturwissenschaftlich-Technische Fakultät, Universität Siegen, D-57068 Siegen, Germany*

<sup>6</sup>*Institut für Quantenoptik, Leibniz Universität Hannover, D-30167 Hannover, Germany*

<sup>7</sup>*Donostia International Physics Center (DIPC), E-20080 San Sebastián, Spain*

<sup>8</sup>*IKERBASQUE, Basque Foundation for Science, E-48011 Bilbao, Spain*

<sup>9</sup>*Institute for Solid State Physics and Optics, Wigner Research Centre for Physics, H-1525 Budapest, Hungary\**

(Dated: January 7, 2022)

We discuss how to detect bipartite entanglement in a Dicke state of many spin-1/2 particles. The particles are split into two subensembles, then collective angular momentum measurements are carried out locally on the two parts. First, we present a bipartite Einstein-Podolsky-Rosen (EPR) steering criterion. Then, we present an entanglement condition that can detect bipartite entanglement in such systems. We demonstrate the utility of the criterion by applying it to a recent experiment given in K. Lange *et al.* [Science **360**, 416 (2018)] realizing a Dicke state in a Bose-Einstein condensate of cold atoms, in which the two subensembles were spatially separated from each other. Our methods also work well if split spin-squeezed states are considered.

## I. INTRODUCTION

Quantum systems with highly correlated internal states, such as spin-squeezed states have been realized in several experiments in Bose-Einstein Condensates (BEC) of two-state atoms [1–6]. Multipartite entanglement has been detected in these states, and it has also been demonstrated that such states are useful for quantum metrology. Recently, Dicke states have also been created in such systems [7, 8]. Beside entanglement, even metrological usefulness of Dicke states has been verified [7, 9]. A Dicke of around 8000 particles has been realized and multipartite entanglement has been detected up to 28 particles within an error a two standard deviation [10, 11]. Moreover, Dicke states of more than 10000 spin-1 atoms and 630-particle entanglement has been detected within an error a single standard deviation [12].

As a next step, it would be important to detect entanglement between two parts of such ensembles, since bipartite entanglement between spatially separated ensembles is the type of entanglement most useful for quantum information processing applications. It has been shown that multipartite entanglement of bosonic two-state atoms can be converted into bipartite entanglement by splitting the ensemble into two [13]. However, is this only a theoretical result or can it be also verified in an experiment, where noise and other imperfections are present? The question is even more timely since the

detection of bipartite entanglement of high-dimensional systems raised a lot of attention [14, 15]. In a recent experiment, bipartite entanglement was successfully detected in a Dicke state created with thousands of atoms and distributed into two spatially separated regions [16].

Another form of quantum correlations, stronger than entanglement, termed Einstein-Podolsky-Rosen (EPR) steering [17–21], has also been recently detected in photonic systems [22], as well as in BEC's [23]. Methods to detect EPR correlations in spatially separated parties, i.e., in a two-well BEC's has also been studied theoretically [24, 25]. Experimentally, the observation of EPR correlations between spatially separated modes was achieved in split-squeezed BEC's [26, 27].

In this paper, we present methods that verify the presence of bipartite entanglement between spatially separated parts of a condensate. These improve the methods given in Ref. [16]. We also introduce a criterion that can verify the presence of steering, by the violation of an EPR steering criterion. Our criteria are particularly well suited for symmetric unpolarized Dicke states given as

$$|D_N\rangle = \binom{N}{N/2}^{-1/2} \sum_k \mathcal{P}_k(|1\rangle^{\otimes N/2} |0\rangle^{\otimes N/2}), \quad (1)$$

where the summation is over all distinct permutations. We will call  $|D_N\rangle$  simply Dicke state in the following. For an equal partitioning of the  $N$  particles, the entanglement of formation of  $|D_N\rangle$  is large, which gives us a strong motivation to try to detect bipartite entanglement in these states [28], see also Appendix A. Our methods also work in other quantum states, such as spin-squeezed states.

\* toth@alumni.nd.edu; <http://www.gtoth.eu>

Our criteria are based on the following uncertainty relation.

**Observation 1.**—For any quantum state, the following number-phase-like uncertainty relation

$$\left( (\Delta J_z)^2 + \frac{1}{4} \right) \frac{(\Delta J_x)^2 + (\Delta J_y)^2}{\langle J_x^2 \rangle + \langle J_y^2 \rangle} \geq \frac{1}{4} \quad (2)$$

holds, we will prove it later in the main text.

Based on the relation Eq. (2), we obtain a criterion that detects entanglement between two parts of the Dicke state in Eq. (1). For that, we divide the system into two subsystems, which we denote by "a" and "b." The corresponding particle numbers in the two subsystems fulfill

$$N_a + N_b = N. \quad (3)$$

In practice, this means that an atomic cloud is spatially separated into two regions as in Fig. 1.

First we present a condition based on steering.

**Observation 2.** We formulate an Einstein-Podolsky-Rosen (EPR) criterion with the angular momentum components as

$$\begin{aligned} & \left[ (\Delta_{\text{inf}} J_z^a)^2 + \frac{1}{4} \right] [(\Delta_{\text{inf}} J_x^a)^2 + (\Delta_{\text{inf}} J_y^a)^2] \\ & \geq \frac{1}{4} (\langle (J_x^a)^2 \rangle + \langle (J_y^a)^2 \rangle), \end{aligned} \quad (4)$$

where  $J_l^a$  and  $J_l^b$  for  $l = x, y, z$  denote the angular momentum components for the two subsystems. Here inference variances are given as

$$(\Delta_{\text{inf}} J_l^a)^2 = [\Delta(J_l^a - J_{l,\text{est}}^a)]^2, \quad (5)$$

where  $J_{l,\text{est}}^a$  are given as

$$J_{l,\text{est}}^a = -g_l J_l^b, \quad (6)$$

for  $l = x, y, z$ , where  $g_l$  are some constants [29]. Any state that violates Eq. (4) is steerable. The inequality in Eq. (4) holds for all non-steerable states, and for all choice of the real parameters  $g_l$ . Therefore, the latter can be optimized in such a way that the violation is maximized, i.e., the left-hand side of Eq. (4) is minimized. We will prove Observation 2 later. We will also show that for an ideal Dicke state of many particles, the optimal choice for  $g_l$  is

$$g_x = g_y = -1, \quad g_z = 1. \quad (7)$$

Note that in order to simplify our notation in the paper, we use  $J_l^a$  and  $J_l^b$  instead of  $J_l^{(a)}$  and  $J_l^{(b)}$ , respectively.

Then, we show a criterion detecting entanglement.

**Observation 3.**—For separable states in bipartite systems

$$\left[ (\Delta J_z)^2 + \frac{1}{4} \right] [(\Delta J_x^-)^2 + (\Delta J_y^-)^2] \geq \frac{\langle J_x^2 + J_y^2 \rangle^2}{N(N+2)} \quad (8)$$

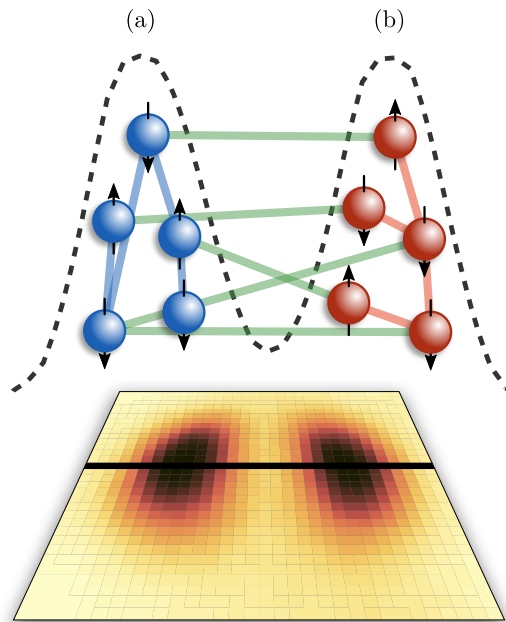


FIG. 1. Entanglement detection between two spatially separated ensembles of spin-1/2 particles. The atomic density profile obtained from an average over 3329 measurements is shown from the experiment presented in Ref. [16].

holds, where we define the difference between the angular momentum components in the two parts as

$$J_l^- = J_l^a - J_l^b \quad (9)$$

for  $l = x, y$ . We will prove Observation 3 later.

If we set the  $g_l$  according to Eq. (7) then the left-hand side of the Eq. (4) is identical to the left-hand side of Eq. (8). Let us compare the right-hand sides. For states that live in the symmetric subspace and for which  $J_z^a, J_z^b \approx 0$ , as we will see later, the right-hand side of Eq. (4) is around 4 times smaller than that of Eq. (8). Thus, for such states, it is more difficult to violate the EPR steering criterion Eq. (4) than the entanglement criterion in Eq. (8), which is consistent with the fact that steering is typically a harder to get resource than entanglement.

In this paper, we will prove the relations mentioned above and show that these relations detect entanglement in a condensate split into two parts. Our method will handle the problem of fluctuating particle numbers, which has two different manifestations. On the one hand, the total particle number varies from experiment to experiment. On the other hand, when the ensemble is split, the particle number in the two subensembles will not be exactly half of the total particle number. Such effects will be handled with an appropriate normalization of the measured quantities.

Our method can also tolerate another imperfection appearing in experiments. While ideally BEC's occupy a single spatial mode, in practice more than one spatial

mode is populated. This is partly due to the fact that BEC's are prepared experimentally at some nonzero temperature. Hence, a quantum state realized with a BEC of two state atoms will never be in a perfectly symmetric state [30]. Such effects have not been considered in many cases when the state of the ensemble was obtained via tomography, and in some cases it was taken into account through ad-hoc methods. We work out criteria that can handle atomic ensembles in not perfectly symmetric states.

Our paper is organized as follows. In Sec. II, we present relevant quantities for the split Dicke state. In Sec. III, we show that the nonzero particle number variance can be handled by an appropriate normalization of the measured quantities. In Sec. IV, we present an EPR steering criterion and an entanglement criterion for Dicke states. In Sec. V, we apply our criteria to various ideal quantum states as well as to an experiment in which a Dicke state has been prepared. Furthermore, we test our criterion numerically also on split spin-squeezed states.

## II. RELEVANT QUANTITIES FOR THE DICKE STATE

Here, we calculate various relevant operator expectation values for the Dicke state, (1). First we consider collective quantities, namely, components of the collective angular momentum and their second moments. Then, we divide the particles into two groups, and calculate collective quantities for the two parts. We obtain the correlations of these quantities, and also the variance of their sum and difference.

All the calculations are interesting, since we can have an understanding what kind of quantities we need to construct an entanglement condition that detects entanglement close to Dicke states. Clearly, we need quantities for which the Dicke state gives an extremal (i.e., minimal or maximal) or almost extremal value.

### A. Collective quantities

In an experiment with ultracold atomic ensembles, we can typically measure only collective quantities. These are the collective angular momentum coordinates defined as

$$J_l = \sum_{n=1}^N j_l^{(n)}, \quad (10)$$

where  $l = x, y, z$ , and  $j_l^{(n)}$  denotes a spin component of the  $n^{\text{th}}$  spin.

Let us now see the expectation values of the collective observables for the Dicke state. First of all, the Dicke state is unpolarized, i.e.,  $\langle J_l \rangle = 0$ . Moreover, it is sym-

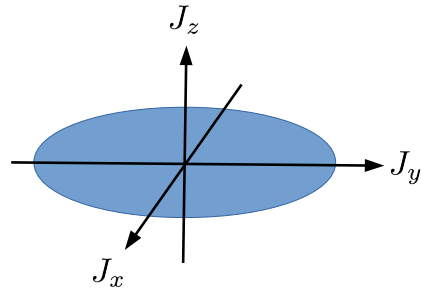


FIG. 2. Uncertainty ellipse of a Dicke state given in Eq. (1). In the  $z$  direction the uncertainty is zero as can be seen from Eq. (12), while in the  $x$  and  $y$  directions it is large, and is given in Eq. (14).

metric under particle exchange, hence

$$\langle J_x^2 + J_y^2 + J_z^2 \rangle = \frac{N}{2} \left( \frac{N}{2} + 1 \right). \quad (11)$$

Since the Dicke state is the eigenstate of  $J_z$ , the variance of the  $z$ -component of the angular momentum is zero

$$\langle J_z^2 \rangle = 0. \quad (12)$$

Finally, the Dicke state is symmetric under rotation around the  $z$  axis. Hence,

$$\langle J_x^\kappa \rangle = \langle J_y^\kappa \rangle \quad (13)$$

for all  $\kappa$ . Equations (11), (12) and (13) lead to

$$\langle J_x^2 \rangle = \langle J_y^2 \rangle = \frac{N}{4} \left( \frac{N}{2} + 1 \right). \quad (14)$$

Thus, the uncertainty ellipse of the collective angular momentum is a ‘‘pancake’’ which has zero width in the  $z$ -direction, while in  $x$  and  $y$ -directions its width is large, as can be seen in Fig. 2.

### B. Bipartite quantities

In order to detect bipartite entanglement in the Dicke state, we divide the ensemble of  $N$  particles into two groups (here without partition noise). The corresponding collective angular momentum components are

$$J_l^a = \sum_{n=1}^{N_a} j_l^{(n)}, \quad J_l^b = \sum_{n=N_a+1}^N j_l^{(n)}. \quad (15)$$

where  $l = x, y, z$ .

Assuming even  $N$ , we introduce the notation

$$N_a = \frac{N}{2} + \delta, \quad N_b = \frac{N}{2} - \delta, \quad (16)$$

where  $-\frac{N}{2} \leq \delta \leq \frac{N}{2}$ . The value  $\delta = 0$  corresponds to dividing the ensemble into two equal halves. The corresponding total spins are

$$j_a = \frac{N}{4} + \frac{\delta}{2}, \quad j_b = \frac{N}{4} - \frac{\delta}{2}. \quad (17)$$

Let us calculate now relevant quantities for the Dicke state split into two halves. For that, we define  $J_l^\pm$  as

$$J_l^\pm = J_l^a \pm J_l^b. \quad (18)$$

We will also use the notation  $J_x \equiv J_x^+$  and  $J_y \equiv J_y^+$ . Let us see now the variances of the quantities defined in Eq. (18). The general rule is

$$\begin{aligned} (\Delta J_l^\pm)^2 &= (\Delta J_l^a)^2 + (\Delta J_l^b)^2 \\ &\mp 2\langle J_l^a \otimes J_l^b \rangle \pm 2\langle J_l^a \rangle \langle J_l^b \rangle, \end{aligned} \quad (19)$$

for  $l = x, y, z$ . Clearly, for the Dicke state, for all expectation values in the two parts we have

$$\langle J_l^s \rangle = 0 \quad (20)$$

for  $l = x, y, z$ . and  $s = a, b$ . Note that here we used the notation  $J_l^s$  instead of  $J_l^{(s)}$  for simplicity.

From Eq. (14), we obtain

$$[\Delta(J_l^a + J_l^b)]^2 = (\Delta J_l)^2 = \frac{N}{4} \left( \frac{N}{2} + 1 \right) \quad (21)$$

for  $l = x, y$ . For large  $N$ , this is about half of the maximum for any quantum state, which is  $N^2/4$ .

The variances of the difference of the angular momentum components of the two parts is

$$\begin{aligned} [\Delta(J_l^a - J_l^b)]^2 &= \frac{N}{8} \frac{N-2}{N-1} + \frac{1}{2} \frac{N}{N-1} \delta^2 \\ &\approx \frac{N}{8} + \frac{1}{2} \delta^2 \end{aligned} \quad (22)$$

for  $l = x, y$ , which is proved in Appendix B. Let us consider the  $\delta = 0$  case separately, for which

$$[\Delta(J_l^a - J_l^b)]^2 \approx \frac{N}{8} \quad (23)$$

holds for  $l = x, y$ . For the fully polarized state  $|1\rangle_z^{\otimes N}$  we get

$$[\Delta(J_l^a - J_l^b)]_{\text{fp},z}^2 = \frac{N}{4} \quad (24)$$

for  $l = x, y$ . The variance in Eq. (23) is smaller than Eq. (24). Note also that if  $\delta$  is nonzero, then  $[\Delta(J_l^a - J_l^b)]^2$  grows rapidly with  $\delta$ , as can be seen from Eq. (22).

Finally, from Eq. (12), we obtain for the variance of the sum of the  $z$ -components

$$[\Delta(J_z^a + J_z^b)]^2 = 0. \quad (25)$$

That is, the variance above is minimal for Dicke states.

### III. HANDLING THE NONZERO VARIANCE OF THE PARTICLES

So far, we assumed that the total particle number  $N$ , and also the particle numbers in the two subsystems,  $N_a$  and  $N_b$  are constants. Similarly, we also assumed that  $j_a$  and  $j_b$  are constants.

In practice, an experiment must be repeated several times in order to obtain sufficient data, and the total particle number is varying from experiment to experiment. Moreover, even if the total particle number  $N$  remained constant, when the condensate is split into two parts, we do not obtain two subensembles with exactly  $N/2$  particles, but the local particle numbers fluctuate due to partition noise. One could in principle postselect experiments with a given particle number, and test entanglement only in the selected experiments. However, apart from requiring single-particle resolution detectors for counting, this approach would result in insufficient statistics to evaluate spin moments. Thus, we need to handle quantum states with fluctuations in the number of particles [30].

In the section we will discuss how to represent a state with particle number fluctuations, how to calculate various quantities after splitting a condensate, and how to introduce a normalization that eliminates some problems arising due to the nonzero particle number variance.

#### A. Description of a quantum state with a nonzero particle number variance

Let us first consider how to represent a quantum state with a nonzero particle number variance. The state of the system can be written as

$$\varrho = \sum_{j_a, j_b} p_{j_a, j_b} \varrho_{j_a, j_b}, \quad (26)$$

where  $\varrho_{j_a, j_b}$  have a definite particle numbers in the two subsystems,  $p_{j_a, j_b} \geq 0$ ,  $\sum_{j_a, j_b} p_{j_a, j_b} = 1$ . Then, expectation values for  $\varrho$  are computed as

$$\langle Af(\hat{j}_a, \hat{j}_b) \rangle_\varrho = \sum_{j_a, j_b} p_{j_a, j_b} \langle A \rangle_{\varrho_{j_a, j_b}} f(j_a, j_b). \quad (27)$$

Here  $f(x, y)$  denotes some two-variable function. The expression  $f(\hat{j}_a, \hat{j}_b)$  depends on the particle number operators  $\hat{N}_a$  and  $\hat{N}_b$  via the relation  $\hat{j}_s = \hat{N}_s/2$  for  $s = a, b$ . On the other hand,  $A$  denotes an operator that does not depend on  $\hat{j}_a$  and  $\hat{j}_b$ . In the following, we will omit "^^" over  $\hat{j}_s$  and  $\hat{N}_s$  for simplicity.

#### B. Bipartite quantities after splitting in an experiment

Let us consider now the splitting that happens in the experiment, which (neglecting the role of particle-particle

interactions) mimics a beam-splitter transformation. We will calculate various expectation values for the Dicke state for that case.

The probability of having  $N/2 + \delta$  particles in subsystem  $a$  is given the binomial formula

$$p_\delta = 2^{-N} \binom{N}{N/2 + \delta}. \quad (28)$$

For an ensemble that on average is split equally, the expectation value of  $\delta$  is zero. However, the number of particles in the two subsystems fluctuate from experiment to experiment. This is described by the variance of the particle number in the subsystem  $a$ , or the variance of  $\delta$  which is

$$\text{var}(N_a) = \text{var}(\delta) = \langle \delta^2 \rangle = \frac{N}{4}. \quad (29)$$

After the correlations, let us see now the collective variance. Based on Eq. (22), they are obtained as

$$\begin{aligned} & [\Delta(J_l^a - J_l^b)]^2 \\ &= \sum_{\delta=-N/2}^{N/2} p_\delta \left( \frac{N}{8} \frac{N-2}{N-1} + \frac{1}{2} \frac{N}{N-1} \delta^2 \right) \\ &= \frac{N}{8} \frac{N-2}{N-1} + \frac{1}{2} \frac{N}{N-1} \text{var}(\delta) = \frac{N}{4} \end{aligned} \quad (30)$$

for  $l = x, y$  [31]. Comparing it to Eq. (23), we can see that the collective variance became around twice larger due to the partition noise appearing during the splitting of the condensate. This is an unwelcome effect, that decreases the quality of the experimental data and makes the detection of correlations in split states more difficult.

Now we present some quantities after the experimental splitting, the derivations are in Appendix C (see also Ref. [31]). The local second moments are

$$\langle (J_x^s)^2 \rangle = \langle (J_y^s)^2 \rangle = \frac{N(N+4)}{32}, \quad (31a)$$

$$\langle (J_z^s)^2 \rangle = \frac{N}{16} \quad (31b)$$

for  $s = a, b$ . The correlations are

$$\langle J_x^a J_x^b \rangle = \langle J_y^a J_y^b \rangle = \frac{N^2}{32}, \quad (32a)$$

$$\langle J_z^a J_z^b \rangle = -\frac{N}{16}. \quad (32b)$$

### C. Bipartite quantities with the normalized spin components

In this section, we consider a normalization of the collective angular momentum components of the subensembles. We calculate some spin expectation values for the Dicke state using a normalization factor, and show that it cancels the effect of the particle number fluctuations.

Concretely, we consider the normalized quantities

$$\mathcal{J}_l^s = J_l^s / \sqrt{j_n(j_n + 1)} \quad (33)$$

for  $l = x, y$  and  $s = a, b$ . Let us also define

$$\mathcal{J}_l^\pm = \mathcal{J}_l^a \pm \mathcal{J}_l^b. \quad (34)$$

For the variance of  $\mathcal{J}_l^-$  we obtain

$$(\Delta \mathcal{J}_l^-)^2 \approx \frac{N}{N^2/2 - \delta^2}, \quad (35)$$

which is shown in Appendix D.

Let us calculate the value for an equal splitting, corresponding to  $\delta = 0$ . We obtain

$$(\Delta \mathcal{J}_l^-)^2 \approx \frac{2}{N}. \quad (36)$$

We now calculate the value taking into account the variance of  $\delta$  while the condensate is split. In this case, the variance of  $\delta$  is given in Eq. (29), hence  $\delta^2 \lesssim N/4$ . In Eq. (35), in the denominator we have

$$N^2/2 \gg \delta^2, \quad (37)$$

if  $N$  is large. Hence, we obtain Eq. (36), the same value we would get for an equal splitting with  $\delta = 0$ . Thus, the fact that particle number variance after splitting is nonzero did not increase the value of the normalized variance. Remember that the corresponding collective variance without a normalization increased a lot due to the nonzero particle number variance during splitting, as can be seen in Eq. (30) when compared to Eq. (23).

Note that we define normalized spin components only for the  $x$  and  $y$  directions only, not in the  $z$  direction. The reason is that the variance of  $[\Delta(J_l^a - J_l^b)]^2$  for  $l = x, y$  depends on the splitting ratio  $x$ , while  $(\Delta J_z)^2$  does not.

## IV. EPR AND ENTANGLEMENT CRITERIA ROBUST TO EXPERIMENTAL IMPERFECTIONS

We first consider a situation in which there are exactly  $N_a$  particles in subsystem  $a$ , and  $N_b$  particles in subsystem  $b$ . Under such circumstances, a quantum state is separable if it can be written as [32]

$$\varrho_{\text{sep}} = \sum_k p_k |\Psi_k^a\rangle \langle \Psi_k^a| \otimes |\Psi_k^b\rangle \langle \Psi_k^b|. \quad (38)$$

If a quantum state cannot be written in this form, then it is entangled.

If the particle numbers  $N_a$  and  $N_b$  fluctuates, then the quantum state can be represented as a mixture of density matrices  $\varrho_{j_a, j_b}$  with a given  $j_a$  and  $j_b$ , as expressed in Eq. (26). The state  $\varrho$  is separable if and only if all  $\varrho_{j_a, j_b}$  are separable [30].

In Appendix E we present some simple entanglement criteria for two spins, which are not yet practical. These need to be improved in the following respects:

(i) In these criteria, we mapped the state of the system into the state of two large spins. However, this is only possible if the quantum states in the two subsystems are in the symmetric subspace. On the experimental side, if the Dicke state lives in a single spatial mode, then in the two subsystems the states are completely symmetric. However, in practice, the Dicke state does not live in a single spatial mode. Hence, we cannot assume perfect symmetry. We have to allow a possibly non-symmetric state of  $N$  spin-1/2 particles.

(ii) The criteria must take into account that the particle number varies from one experimental realization to the other. Even if the total particle number is kept constant, the particle numbers in the two subsystems will vary in each realization because of partition noise, as described in Sec. III B. This can make some of the correlators entering the entanglement criteria worse, such as in the case of Appendix E 2. This effect can be compensated by appropriate normalization of the angular momentum coordinates, as we have introduced in Sec. III C.

(iii) In general, the criterion must be robust enough to detect entanglement in an actual experiment. There, the variance of  $(\Delta J_z)^2$  can be very close to zero. On the other hand,  $[\Delta(J_x^a - J_x^b)]^2 + [\Delta(J_y^a - J_y^b)]^2$  can be much larger than for the ideal Dicke state (see later Sec. V B). Hence, an entanglement criterion with the product of these two quantities could be more efficient than a criterion with their sum.

We will now present such an entanglement criterion, based on the number-phase-like uncertainty relation given in Eq. (2).

### A. Number-phase-like uncertainty

Here, we derive an uncertainty relation particularly suited for Dicke states, and for deriving entanglement and EPR steering criteria.

*Proof of Observation 1.*—We start from the Heisenberg uncertainty relations

$$\begin{aligned} (\Delta J_z)^2 (\Delta J_x)^2 &\geq \frac{1}{4} \langle J_y \rangle^2, \\ (\Delta J_z)^2 (\Delta J_y)^2 &\geq \frac{1}{4} \langle J_x \rangle^2. \end{aligned} \quad (39)$$

By summing the two inequalities we obtain

$$(\Delta J_z)^2 [(\Delta J_x)^2 + (\Delta J_y)^2] \geq \frac{1}{4} (\langle J_x \rangle^2 + \langle J_y \rangle^2). \quad (40)$$

Then, by adding  $[(\Delta J_x)^2 + (\Delta J_y)^2]/4$  to both sides, and dividing by  $\langle J_x^2 \rangle + \langle J_y^2 \rangle$ , we arrive at Eq. (2). ■

Equation (2) is similar to a number-phase uncertainty-like relation [33]. In Eq. (2), the first factor represents the fluctuations in the particle number difference and the

second term represents the fluctuations in the phase difference. In Appendix F, we show how Eq. (2) can be connected to the literature on number-phase uncertainties.

It is interesting to ask why the term  $(\Delta J_z)^2$  in Eq. (2) has also a constant part. This is because  $(\Delta J_z)^2$  can be zero. If there were not a constant included in the first, then the second term would be infinite in this case, which is impossible. Due to the constant term, a state with  $(\Delta J_z)^2 = 0$  saturates the relation given in Eq. (2) if the second term is 1.

### B. Einstein-Podolsky-Rosen criterion

In this section, we derive a criterion for steering given in Eq. (4). The idea follows the same approach used to derive Eq. (2). We will also derive a form that uses normalized spin components given in Eq. (33), which make it more resistant to the particle number variance.

An important EPR condition with these operators is given as [34–36]

$$(\Delta_{\text{inf}} J_z^a)^2 (\Delta_{\text{inf}} J_y^a)^2 \geq \frac{1}{4} |\langle J_x^a \rangle|^2, \quad (41)$$

where the right-hand side can be improved considering an inferred value  $\langle J_x^a \rangle$  based on measurements on party  $b$  [21]. These relations are tailored for states that have a spin almost fully polarized in the  $x$ -direction.

*Proof of Observation 2.*—We start directly from the uncertainty relation Eq. (2). Using that for all non-steerable states [18–21]

$$(\Delta_{\text{inf}} O^a)^2 \geq (\Delta O^a)^2, \quad (42)$$

we arrive at Eq. (4). ■

The gain factors  $g$  [see Eq. (6)] appear only in the inferred variances, and not in the bound as it happens for entanglement criteria (see e.g., Eq. (1) of Ref. [26]). Therefore, to minimize the criterion it is enough to minimize each inferred variance independently. This is done by taking the derivative with respect to  $g$ , and then equating to zero. This straightforward calculation gives

$$g_l = -\frac{\text{Cov}(J_l^a, J_l^b)}{(\Delta J_l^b)^2}, \quad (43)$$

where the covariance is defined as

$$\text{Cov}(J_l^a, J_l^b) = \langle J_l^a J_l^b \rangle - \langle J_l^a \rangle \langle J_l^b \rangle. \quad (44)$$

Based on Eq. (43), (32a) and (31a), the optimal gain factors for 50:50 split Dicke states are

$$g_x = g_y = -N/(N+4), \quad g_z = 1. \quad (45)$$

For large  $N$ , these coincides with Eq. (7), which are the values we can consider for simplicity as in typical experiments we have  $N \gg 100$ .

Next, we will derive a criterion similar to Eq. (4), but with normalized spin operators. We estimate the measurement results on subsystem  $a$  based on measurements on subsystem  $b$  as

$$J_{z,\text{est}}^a = -J_z^b, \quad (46)$$

For estimating the measurement results in the  $x$  and  $y$  components of the angular momentum, we use

$$J_{l,\text{est}}^a = +\sqrt{\frac{j_a(j_a+1)}{j_b(j_b+1)}} J_l^b, \quad (47)$$

for  $l = x, y$ . Plugging Eq. (47) into Eq. (4), we arrive at a relation with normalized quantities.

**Observation 4.**—The following EPR steering criterion holds with the normalized quantities

$$\begin{aligned} & \left[ (\Delta J_z)^2 + \frac{1}{4} \right] [(\Delta \mathcal{J}_x^-)^2 + (\Delta \mathcal{J}_y^-)^2] \\ & \geq \frac{1}{4} \langle (\mathcal{J}_x^a)^2 + (\mathcal{J}_y^a)^2 \rangle. \end{aligned} \quad (48)$$

and can be used for Dicke states. A more general form is given as

$$\begin{aligned} & \left\{ [\Delta(J_z^a - J_{z,\text{est}}^b)]^2 + \frac{1}{4} \right\} \\ & \times \left\{ [\Delta(\mathcal{J}_x^a - \mathcal{J}_{x,\text{est}}^b)]^2 + [\Delta(\mathcal{J}_y^a - \mathcal{J}_{y,\text{est}}^b)]^2 \right\} \\ & \geq \frac{1}{4} \langle (\mathcal{J}_x^a)^2 + (\mathcal{J}_y^a)^2 \rangle. \end{aligned} \quad (49)$$

If we substitute the  $J_{l,\text{est}}^a$  defined in Eqs. (46) and (47) into Eq. (49), we obtain Eq. (48).

### C. Entanglement criterion

In this section, we prove our entanglement criterion given in Eq. (8). We also present a version of the criterion with normalized spin operators.

**Observation 5.**—An entanglement criterion with a bound depending on squared first-moments of the collective spin is

$$(\Delta J_z)^2 [(\Delta J_x^-)^2 + (\Delta J_y^-)^2] \geq \frac{1}{4} (\langle J_x \rangle^2 + \langle J_y \rangle^2), \quad (50)$$

where  $J_l^\pm$  is defined in Eq. (18).

*Proof.* Eq. (16) of Ref. [37] shows that for all separable states

$$[\Delta(U_a \pm U_b)]^2 [\Delta(V_a \pm V_b)]^2 \geq \frac{1}{4} (|\langle C_a \rangle| + |\langle C_b \rangle|)^2 \quad (51)$$

holds, where  $U_s$  and  $V_s$  for  $s = a, b$  are operators acting on the two subsystems, and  $C_s = i[U_s, V_s]$ . We will now use that  $(|x| + |y|)^2 \geq (x + y)^2$  for any  $x, y$ . Hence, from Eq. (52) follows

$$[\Delta(U_a + U_b)]^2 [\Delta(V_a - V_b)]^2 \geq \frac{1}{4} (\langle C_a \rangle + \langle C_b \rangle)^2. \quad (52)$$

We use Eq. (52) for  $U_s = J_z^s$  and  $V_s = J_x^s$ , and for  $U_s = J_z^s$  and  $V_s = J_y^s$  to obtain two inequalities valid for separable states. Finally, we sum these two inequalities, and we obtain Eq. (50). ■

The criterion presented in Eq. (50) cannot be used for Dicke states, as it has first moments of the angular momentum coordinates on the right-hand side, which are zero for such states. Therefore, we will now derive criteria that work for Dicke states as well.

**Observation 6.**—For all separable states

$$\left[ (\Delta J_z)^2 + \frac{1}{4} \right] [(\Delta J_x^-)^2 + (\Delta J_y^-)^2] \geq \frac{1}{4} \left\langle \sqrt{J_x^2 + J_y^2} \right\rangle^2 \quad (53)$$

holds.

*Proof.*—Let us start from Eq. (50), which is true for all separable states. We add to both sides

$$\frac{1}{4} [(\Delta J_x^+)^2 + (\Delta J_y^+)^2]. \quad (54)$$

We obtain the inequality

$$\begin{aligned} & (\Delta J_z)^2 [(\Delta J_x^-)^2 + (\Delta J_y^-)^2] + \frac{1}{4} [(\Delta J_x^+)^2 + (\Delta J_y^+)^2] \\ & \geq \frac{1}{4} (\langle J_x^2 \rangle + \langle J_y^2 \rangle). \end{aligned} \quad (55)$$

Now, let us consider only product states. For these,

$$\begin{aligned} & (\Delta J_x^+)^2 + (\Delta J_y^+)^2 \\ & = (\Delta J_x^-)^2 + (\Delta J_y^-)^2 \\ & = (\Delta J_x^a)^2 + (\Delta J_x^b)^2 + (\Delta J_y^a)^2 + (\Delta J_y^b)^2 \end{aligned} \quad (56)$$

holds. Based on Eqs. (55) and (56), for product states

$$\left[ (\Delta J_z)^2 + \frac{1}{4} \right] [(\Delta J_x^-)^2 + (\Delta J_y^-)^2] \geq \frac{1}{4} \langle J_x^2 + J_y^2 \rangle \quad (57)$$

holds. Equation (57) is not necessarily true for separable states since the left-hand side is not concave in the state.

Let us consider another equation that is true for product states, namely Eq. (53), which follows from Eq. (57) and from that for any observable  $A$

$$\langle A \rangle \geq \langle \sqrt{A} \rangle^2 \quad (58)$$

holds. We claim that Eq. (53) is also true for all separable states. Let us reformulate Eq. (53) as

$$x^2 y^2 \geq c^2, \quad (59)$$

where we define  $x, y$  and  $c$  as

$$\begin{aligned} x^2 &= \alpha \left[ (\Delta J_z)^2 + \frac{1}{4} \right], \quad y^2 = \beta [(\Delta J_x^-)^2 + (\Delta J_y^-)^2], \\ c &= \frac{1}{2} \sqrt{\alpha \beta} \left\langle \sqrt{J_x^2 + J_y^2} \right\rangle, \end{aligned} \quad (60)$$

and  $\alpha, \beta > 0$ . Then, from Eq. (59) and  $x^2 + y^2 \geq 2xy$  follows that [37]

$$x^2 + y^2 \geq 2c. \quad (61)$$

Based on Eq. (60), the inequality in Eq. (61) can be written as

$$\alpha \left[ (\Delta J_z)^2 + \frac{1}{4} \right] + \beta [(\Delta J_x^-)^2 + (\Delta J_y^-)^2] \geq \sqrt{\alpha\beta} \left\langle \sqrt{J_x^2 + J_y^2} \right\rangle. \quad (62)$$

So far we know that Eq. (62) is true for product states for any choice of the real coefficients  $\alpha$ 's and  $\beta$ 's. However, the left-hand side of Eq. (62) is concave, the right-hand side is linear in  $\varrho$ . Hence, it is also valid for separable states.

One can also see that Eq. (62) corresponds to the tangents of the hyperbola appearing in Eq. (53). Let us consider all the inequalities that can be obtained from Eq. (62) for all  $\alpha$ 's and  $\beta$ 's. They are all fulfilled if and only if Eq. (53) is fulfilled. Hence, Eq. (53) is also valid for all separable states. ■

Equation (53) is an entanglement condition that detects the Dicke state given in Eq. (1) as entangled. However, on the right-hand side we have the expectation value of  $\sqrt{J_x^2 + J_y^2}$ , which is difficult to measure in an experiment. We now show somewhat weaker criteria, in which the operator expectation values on the right-hand side are easy to measure.

*Proof of Observation 3.*—We use that for  $A \geq 0$  we have

$$\langle \sqrt{A} \rangle \geq \langle A \rangle / \sqrt{\lambda_{\max}(A)}. \quad (63)$$

In our case, the operator  $A$  is given as

$$A = J_x^2 + J_y^2 \quad (64)$$

and for this operator the maximal eigenvalue is

$$\lambda_{\max}(A) = N(N+2)/4. \quad (65)$$

Hence, the right-hand side of Eq. (53) is never smaller than that of Eq. (8). ■

We present another condition, also related to Eq. (53).

**Observation 6.**—The following holds for all separable states

$$\left[ (\Delta J_z)^2 + \frac{1}{4} \right] [(\Delta J_x^-)^2 + (\Delta J_y^-)^2] \geq \frac{1}{8} (\langle |J_x| \rangle + \langle |J_y| \rangle)^2. \quad (66)$$

Here,  $\langle |A| \rangle$  is measured as follows. We measure  $A$  and compute the absolute value. Then, we measure the average of these absolute values.

*Proof.* The inequality

$$\sqrt{\frac{x^2 + y^2}{2}} \geq \frac{\sqrt{x^2} + \sqrt{y^2}}{2} \quad (67)$$

holds for numbers  $x$  and  $y$ , since the square root is concave. An analogous relation is true for matrices, since the square root is matrix concave. Hence,

$$\sqrt{J_x^2 + J_y^2} \geq \frac{\sqrt{J_x^2} + \sqrt{J_y^2}}{\sqrt{2}} \equiv \frac{|J_x| + |J_y|}{\sqrt{2}}, \quad (68)$$

which finishes the proof. ■

Next, we present the criteria derived in this section with normalized spin components. These are more resistant to particle number fluctuations (see Sec. III C), and are thus better for an experimental use. They can be derived repeating the steps described in this section, after the normalization is inserted in the formulas.

**Observation 7.**—The normalized version of Eq. (8) is

$$\left[ (\Delta J_z)^2 + \frac{1}{4} \right] [(\Delta \mathcal{J}_x^-)^2 + (\Delta \mathcal{J}_y^-)^2] \geq \frac{1}{16} \langle \mathcal{J}_x^2 + \mathcal{J}_y^2 \rangle^2, \quad (69)$$

*Proof.* We start from the normalized version of Eq. (53). Then, we have to apply Eq. (63) to get rid of the square root within the expectation value. ■

**Observation 8.**—The normalized version of Eq. (66) is

$$\left[ (\Delta J_z)^2 + \frac{1}{4} \right] [(\Delta \mathcal{J}_x^-)^2 + (\Delta \mathcal{J}_y^-)^2] \geq \frac{1}{8} (\langle |\mathcal{J}_x| \rangle + \langle |\mathcal{J}_y| \rangle)^2. \quad (70)$$

*Proof.* We start from the normalized version of Eq. (66). Then, we have to apply Eq. (68) to get rid of the square root within the expectation value. ■

The left-hand sides of Eq. (48) and Eq. (69) are identical. Let us compare the right-hand sides. For states that live in the symmetric subspace and for which  $(\Delta J_z)^2 \approx 0$ , the right-hand side of Eq. (48) is around 4 times smaller than that of Eq. (69). Thus, for such states, it is more difficult to violate the EPR steering criterion Eq. (48) than the entanglement criterion in Eq. (69). Again, this reflects the fact that steering is a stronger form of quantum correlations than entanglement.

## V. APPLICATION OF THE ENTANGLEMENT CRITERION FOR VARIOUS QUANTUM STATES

In this section, we examine how our EPR steering criterion and entanglement criterion work for various ideal quantum states, as well as for states prepared experimentally.

### A. Testing EPR steering and entanglement for various quantum states

We calculate the relevant normalized quantities for the EPR steering criterion given in Eq. (49) and entanglement criterion given in Eq. (69) for various quantum states. The results for the EPR condition are shown in Table I. The quantities presented in the table are the sum of variances in subsystem  $a$

$$V_a := [\Delta(\mathcal{J}_x^a - \mathcal{J}_{x,\text{est}}^a)]^2 + [\Delta(\mathcal{J}_y^a - \mathcal{J}_{y,\text{est}}^a)]^2, \quad (71)$$

and the sum of second moments in subsystem  $a$

$$E_a := \langle (\mathcal{J}_x^{(a)})^2 \rangle + \langle (\mathcal{J}_y^{(a)})^2 \rangle. \quad (72)$$



Quantum state	$[\Delta(J_z^a - J_{z,\text{est}}^a)]^2$	$V_a$	$E_a$	LHS/RHS
$ D_N\rangle$	0	$4/N$	1	$4/N$
$ +1/2\rangle_z^{\otimes N}$	0	$4/N$	$4/N$	1
$ +1/2\rangle_x^{\otimes N}$	$N/8$	$2/N$	1	1
$ D_{N/2}\rangle \otimes  D_{N/2}\rangle$	0	1	1	1

TABLE I. Approximate values for large  $N$  of the relevant quantities for the EPR steering criterion given in Eq. (49) for various quantum states. Some of the quantities presented in the table are defined in Eqs. (71) and (72), while the EPR condition with those is given in (73). In the last column, the left-hand side divided by the right-hand side of (73) is given. A value smaller than one indicates that the state violates the criterion given in Eq. (49). A value close to one means that the state is close to saturate the relation.

Quantum state	$(\Delta J_z)^2$	$V$	$E$	LHS/RHS
$ D_N\rangle$	0	$4/N$	4	$1/N$
$ +1/2\rangle_z^{\otimes N}$	0	$8/N$	$8/N$	$N/2$
$ +1/2\rangle_x^{\otimes N}$	$N/4$	$4/N$	4	1
$ D_{N/2}\rangle \otimes  D_{N/2}\rangle$	0	2	2	2

TABLE II. Approximate values for large  $N$  of the relevant quantities for the entanglement criterion given in Eq. (69) for various quantum states. Some of the quantities presented in the table are defined in Eqs. (74) and (75), while the entanglement condition with those is given in (76). In the last column the left-hand side divided by the right-hand side of (76) is given. A value smaller than one indicates that the state violates the criterion given in Eq. (69). A value close to one means that the state is close to saturate the relation.

The criterion given in Eq. (49) can be written as

$$\{[\Delta(J_z^a - J_{z,\text{est}}^a)]^2 + 1/4\}V_a \geq E_a/4 \quad (73)$$

with the quantities given in the table.

The results for the entanglement condition are shown in Table II. The quantities presented in the table are the variances of the differences between the two subsystems

$$V := (\Delta\mathcal{J}_x^-)^2 + (\Delta\mathcal{J}_y^-)^2, \quad (74)$$

and the sum of global second moments

$$E := \langle\mathcal{J}_x^2\rangle + \langle\mathcal{J}_y^2\rangle, \quad (75)$$

The criterion given in Eq. (69) can be written as

$$[(\Delta J_z)^2 + 1/4]V \geq E^2/16 \quad (76)$$

with the quantities given in the table.

The Dicke state violates both criteria very strongly. The state with all states pointing into the  $x$ -direction is close to saturate both relations. All examples are valid when the ensemble is divided with the experimental procedure and also for the case when the ensemble is divided

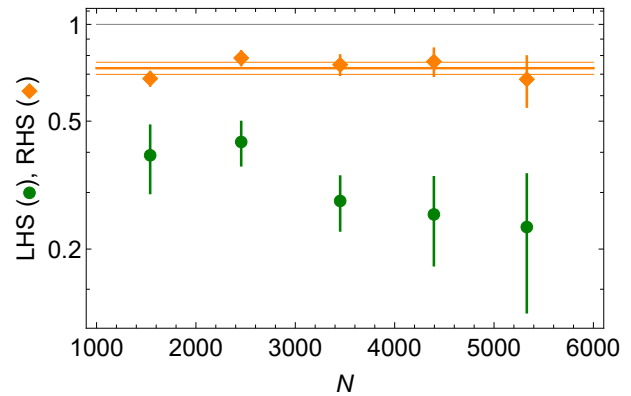


FIG. 3. Entanglement detection between two spatially separated particle ensembles. (orange) Right-hand side of the entanglement criterion given in Eq. (69). (green) Left-hand side of Eq. (69).

into two equal halves. Since we use the normalized quantities, there is not an observable difference. For Eqs. (71) and (73), for the Dicke state, we used

$$\mathcal{J}_{x,\text{est}}^a = \mathcal{J}_x^b, \quad \mathcal{J}_{y,\text{est}}^a = \mathcal{J}_y^b, \quad J_{z,\text{est}}^a = -J_z^b. \quad (77)$$

The other states were product states, hence we used

$$\mathcal{J}_{x,\text{est}}^a = \mathcal{J}_{y,\text{est}}^a = J_{z,\text{est}}^a = 0. \quad (78)$$

## B. Experimental results

Next, we test our entanglement criterion in an experiment. We use the experimental data from Ref. [16]. There, a Dicke state, (1), of around 8000 atoms was prepared, and bipartite entanglement was detected after splitting. However in that work, a different entanglement criterion was used.

Due to the characteristics of the setup, they could measure  $J_z^s$  in the two subsystems. They could also measure

$$J_\alpha^s = J_x^s \cos(\alpha) + J_y^s \sin(\alpha), \quad (79)$$

where  $s = a, b$ , and  $\alpha$  is a random angle equally distributed between 0 and  $2\pi$ . Note that at a given measurement, the  $\alpha$  angle is the same for  $J_\alpha^a$  and  $J_\alpha^b$ .

Let us now consider the normalized single-subsystem quantity

$$\mathcal{J}_\alpha^s = J_\alpha^s / \sqrt{j_n(j_n + 1)} \quad (80)$$

and the normalized two subsystem quantity

$$\mathcal{J}_\alpha^\pm = \mathcal{J}_\alpha^a \pm \mathcal{J}_\alpha^b. \quad (81)$$

The average  $m^{\text{th}}$  moment of the angular momentum in the  $x - y$  plane is defined as

$$\langle(\mathcal{J}_\perp^\pm)^m\rangle = \frac{1}{2\pi} \int_{\alpha=0}^{2\pi} \langle(\mathcal{J}_\alpha^\pm)^m\rangle. \quad (82)$$

It is easy to see that the average second moment can be expressed as an average of two operators, rather than with an integral as

$$\langle (\mathcal{J}_\perp^m)^2 \rangle = \frac{\langle (\mathcal{J}_x^m)^2 + (\mathcal{J}_y^m)^2 \rangle}{2} \quad (83)$$

for  $m \in \{+, -\}$ , while the first moment is zero

$$\langle \mathcal{J}_\perp^m \rangle = 0. \quad (84)$$

Equation (83) can be shown noting the relation for the second moments

$$\frac{1}{2\pi} \int_{\alpha=0}^{2\pi} d\alpha (J_\alpha^s)^2 = \frac{(J_x^s)^2 + (J_y^s)^2}{2}, \quad (85)$$

and another one for the correlations

$$\frac{1}{2\pi} \int_{\alpha=0}^{2\pi} d\alpha (J_\alpha^a J_\alpha^b) = \frac{J_x^a J_x^b + J_y^a J_y^b}{2}, \quad (86)$$

which can be proven with straightforward algebra.

With these, the entanglement criterion given in Eq. (69) can be rewritten as

$$\left[ (\Delta J_z)^2 + \frac{1}{4} \right] [2(\Delta \mathcal{J}_\perp^-)^2] \geq \frac{1}{16} \langle (\mathcal{J}_\perp^+)^2 \rangle. \quad (87)$$

In the experiment described in Ref. [16], they used as point of reference the values obtained for the state fully polarized in the  $x$ -direction given as

$$(\Delta J_z)_{\text{fp},x}^2 = \frac{N}{4}, \quad (\Delta \mathcal{J}_\perp^-)_{\text{fp},x}^2 = \frac{2}{N}. \quad (88)$$

In Table II it can be seen that this state is very close to saturate the entanglement criterion Eq. (69) for large  $N$ . In the experiment described in Ref. [16],  $(\Delta J_z)^2$  is much smaller than  $(\Delta J_z)_{\text{fp},x}^2$ . The reason is that the process that prepares the Dicke state ideally creates the eigenstate of  $J_z$  with eigenvalue 0, that is, ideally we have  $(\Delta J_z)^2 = 0$ . On the other hand,  $\langle (\mathcal{J}_\perp^-)^2 \rangle$  is larger than  $(\Delta \mathcal{J}_\perp^-)_{\text{fp},x}^2$ . The state is close to be symmetric. We plotted the results in Fig. 3. We can see that the experimental values violate the condition given in Eq. (87). The method presented in this paper is somewhat more sensitive than the one presented in Ref. [16].

Let us examine now, how the EPR steering criterion given in Eq. (48) could be used in a setup similar to the experiment of Ref. [16]. For that, we define average  $m^{\text{th}}$  moment of the angular momentum in the  $x - y$  plane is defined as

$$\langle (\mathcal{J}_\perp^a)^m \rangle = \frac{1}{2\pi} \int_{\alpha=0}^{2\pi} \langle (\mathcal{J}_\alpha^a)^m \rangle. \quad (89)$$

We obtain the relation

$$\left[ (\Delta J_z)^2 + \frac{1}{4} \right] [2(\Delta \mathcal{J}_\perp^-)^2] \geq \frac{1}{4} \langle (\mathcal{J}_\perp^a)^2 \rangle. \quad (90)$$

The experimental data of Ref. [16] are not violating the EPR steering criterion Eq. (90), but they are not far from it. For instance, for 5300 atoms LHS=  $0.23 \pm 0.11$  and RHS=  $0.20 \pm 0.20$  is obtained.

### C. Application of the entanglement condition for split spin-squeezed states

From Sec. V A we could see that the state fully polarized in the  $x$ -direction was close to saturate the entanglement criterion Eq. (69). Now, if we start from this state, and apply some suitable interaction between the particles, we can obtain a spin-squeezed state, which has a reduced uncertainty along some direction orthogonal to the mean spin. Such states are entangled, and they are useful, *e.g.*, for quantum metrology, where they outperform separable states [38–40]. Spin-squeezed states are now routinely prepared in experiments, and their entanglement has been detected in cold atomic ensembles [41–44] and in BEC's [1, 2, 4–6]. In addition, collective measurements allowed to detect and quantify even Bell correlations in such states [45–48]. On the other hand, the use of local spin measurements in BEC's allowed to detect entanglement and EPR steering between parts of a spin-squeezed state [25, 26].

Here we show that our entanglement criterion detects bipartite entanglement in split spin-squeezed states. Such states can be created starting from a spin coherent state polarized along the  $x$ -direction. Then, we apply a dynamics governed by the one-axis twisting Hamiltonian

$$H = \chi J_z^2, \quad (91)$$

where  $\chi$  defines the interaction strength. The state can be parametrized during the evolution by the adimensional parameter  $\mu = 2\chi t$ , where  $t$ , is the evolution time. With this parametrization we follow the notation of Ref. [38]. The state has a reduced spin variance along some direction in the  $yz$  plane. By applying a rotation around the  $x$ -axis, we can orient the state such that the variance is smallest along the  $z$  direction.

Let us now consider a splitting of the state into two halves with equal average particle number, and investigate correlations between them. The calculations can be simplified since the state is in the symmetric subspace. The resulting bipartite state has been presented in Ref. [25], and it allows us to evaluate analytically Eq. (49), see Fig. 4. By comparing the violation of the Reid criterion for spins, Eq. (41), and of the entanglement criterion presented in this paper, Eq. (49), we observe that the latter allows us to detect steering for a wider class of states.

In Fig. 5, we show similar curves for the entanglement criterion given in Eq. (69). We compare our approach to the criterion, which is based on the paper of Giovannetti *et al.* given in Ref. [37] (see also Ref. [25]). We can see that our criterion allows us to detect spin-squeezed states as entangled even for large  $\mu$  values where the state is significantly non-Gaussian.

In these calculations, we considered a symmetric splitting of the state and criteria with normalization, Eq. (49) and Eq. (69). In summary, our criteria for bipartite entanglement developed for the unpolarized Dicke state work also for other classes of states, such as spin-squeezed

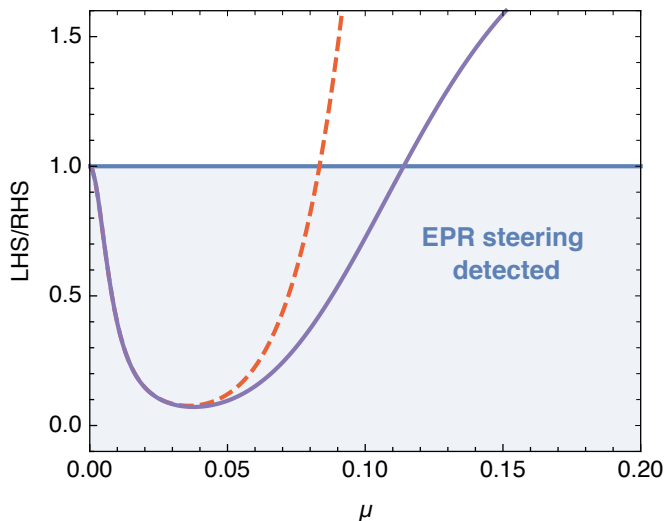


FIG. 4. Detection of EPR steering in a split spin-squeezed state with  $N = 500$  particles and squeezing strength  $\mu$  (see main text). (solid) Left-hand side divided by the right-hand side for the EPR criterion given in Eq. (49). (dashed) Left-hand side divided by the right-hand side for the EPR criterion given in Eq. (41), which is based on the Reid criterion for spins given in Refs. [34–36]. Values below 1 signal the presence of EPR steering. In both cases the gain factors  $g$  have been set to their optimal value Eq. (43).

states. Note that this is similar to the criteria for multipartite entanglement developed for Dicke states in Ref. [10], that were also applicable for spin-squeezed states [11].

## CONCLUSIONS

We presented methods to detect Einstein-Podolsky-Rosen steering and a bipartite entanglement. They are based on a simple uncertainty relation resembling a number-phase uncertainty for spin systems. Our methods are especially suited for Dicke states, which gave the motivation for this work, however, they can be also applied to other experimentally relevant states, for instance, split spin-squeezed states. Our methods can handle imperfections, such as not perfectly symmetric states and a nonzero particle number variance. The entanglement condition presented is somewhat simpler and seems to be stronger than the relation given in Ref. [16]. When applied to split nonclassical states, all these conditions need collective spin measurements in the two halves of the system.

## ACKNOWLEDGMENTS

We thank G. Colangelo, O. Gühne, P. Hyllus, M. W. Mitchell, and J. Peise for discussions. We acknowl-

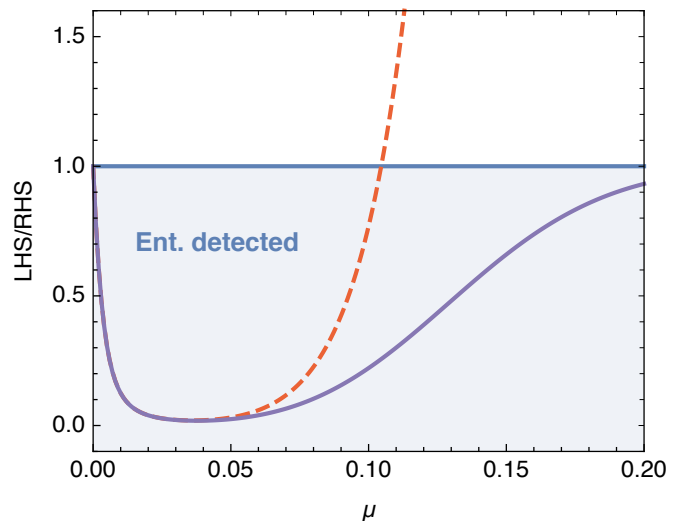


FIG. 5. Detection of entanglement in a split spin-squeezed state with  $N = 500$  particles and squeezing strength  $\mu$  (see main text). (solid) Left-hand side divided by the right-hand side for the entanglement criterion given in Eq. (69). (dashed) Left-hand side divided by the right-hand side for the entanglement criterion proposed by Giovannetti *et al.* in Ref. [37], and analyzed in Ref. [25]. Values below 1 signal the presence of entanglement.

edge the support of the EU (COST Action CA15220, QuantERA CEBBEC), the Spanish MCIU (Grant No. PCI2018-092896), the Spanish Ministry of Science, Innovation and Universities and the European Regional Development Fund FEDER through Grant No. PGC2018-101355-B-I00 (MCIU/AEI/FEDER, EU), the Basque Government (Grant No. IT986-16), and the National Research, Development and Innovation Office NKFIH (Grant No. K124351, No. KH129601). We thank the "Frontline" Research Excellence Programme of the NKFIH (Grant No. KKP133827). G.T. thanks a Bessel Research Award of the Humboldt Foundation. The work is funded by the Deutsche Forschungsgemeinschaft (DFG, German Research Foundation) under Germany's Excellence Strategy (EXC-2123 QuantumFrontiers 390837967), and through CRC 1227 (DQ-mat), project A02. M. F. was partially supported by the Research Fund of the University of Basel for Excellent Junior Researchers. We also thank the Deutsche Forschungsgemeinschaft (DFG, German Research Foundation, Project No. 447948357), the ERC (Consolidator Grant 683107/TempoQ) G.V. acknowledges support from the Austrian Science Fund (FWF) through projects ZK 3 (Zukunftskolleg) and M 2462-N27 (Lise-Meitner).

## Appendix A: The Dicke state as a bipartite state

In this Appendix, we analyze the entanglement properties of Dicke states given in Eq. (1). Dicke state have

been realized with photons and trapped ions for up to 6 particles, using parametric down conversion [49–51]. Later, large Dicke states have been created with BEC of two-state atoms [7, 8, 10–12]. The entanglement of Dicke states is quite robust to external noise and imperfections. For instance, losing a particle does not make the Dicke state separable. Dicke states make possible quantum metrology with the maximal, Heisenberg scaling [7].

The entanglement of formation of  $|D_N\rangle$  is known considering an equal partitioning of the  $N$  particles [28]. For large  $N$ , it is given as

$$E_F^{(\text{Dicke})} \approx \log_2(N)/2. \quad (\text{A1})$$

In comparison, the entanglement of a maximally entangled states of qudits of dimension  $d$  is  $\log_2 d$ . Hence, the bipartite entanglement of the Dicke states is close to the entanglement of a maximally entangled state with  $d = \sqrt{N}$ .

Let us now analyze the bipartite entanglement of Dicke states. The Schmidt decomposition of the Dicke is [28, 52]

$$|D_N\rangle = \sum_{m=0}^N \lambda_m |m, N_a\rangle \otimes |N/2 - m, N_b\rangle, \quad (\text{A2})$$

where the coefficients are

$$\lambda_m = \binom{N}{N_a}^{-\frac{1}{2}} \left[ \binom{N_a}{m} \binom{N_b}{N/2 - m} \right]^{\frac{1}{2}} \quad (\text{A3})$$

and the basis states in the two subsystems are

$$|m, N\rangle = \binom{N}{m}^{-1/2} \sum_k \mathcal{P}_k(|1\rangle^{\otimes m} |0\rangle^{\otimes N-m}). \quad (\text{A4})$$

The states given in Eq. (A4) are symmetrized superpositions of all product states with  $m$  1's and  $N - m$  0's.

Let us now consider an equal splitting, which means

$$N_a = N_b = \frac{N}{2}. \quad (\text{A5})$$

While the state has  $N + 1$  nonzero Schmidt coefficients, most of these coefficients are close to zero since for large  $N$  the binomial can be approximated with a Gaussian and we obtain

$$\lambda_m \propto e^{-\frac{(m-N/2)^2}{2(N/4)}}. \quad (\text{A6})$$

Hence,  $\lambda_m$  is large if

$$|m - N/2| \lesssim \frac{\sqrt{N}}{2}. \quad (\text{A7})$$

This explanation made it easier to understand Eq. (A1) qualitatively.

It is instructive to compare Dicke states to the celebrated Greenberger-Horne-Zeilinger (GHZ) states [53]

$$|\text{GHZ}_N\rangle = \frac{1}{\sqrt{2}} (|0\rangle^{\otimes N} + |1\rangle^{\otimes N}), \quad (\text{A8})$$

which play a central role in quantum information science. GHZ states have been realized in photonic systems [54–58] and in cold trapped ions [59–61]. GHZ states make possible quantum metrology with the maximal, Heisenberg scaling [59].

GHZ states have a bipartite entanglement of the two halves of the particles equal to

$$E_F^{(\text{GHZ})} = \log_2 2 = 1. \quad (\text{A9})$$

Moreover, the entanglement of GHZ states is fragile, and the loss of a single particle can lead to a trivial separable state. GHZ states have been created successfully up to 10-20 particles.

## Appendix B: Derivation of Eq. (22)

In this Appendix, we calculate various quantities for the Dicke state given in Eq. (1). We obtain two-particle and bipartite correlations, and at the end we derive Eq. (22).

We will now calculate two-particle correlations of the Dicke state. Due to the permutational invariance of the Dicke state

$$\langle j_l^{(1)} j_l^{(2)} \rangle = \langle j_l^{(n)} j_l^{(m)} \rangle \quad (\text{B1})$$

holds for  $l = x, y, z$  and for all  $n \neq m$ . Hence,

$$\langle J_l^2 \rangle = \frac{N}{4} + N(N-1) \langle j_l^{(1)} j_l^{(2)} \rangle. \quad (\text{B2})$$

Then, based on Eqs. (14) and (B2)

$$\langle j_l^{(1)} j_l^{(2)} \rangle = \frac{1}{8} \frac{N}{N-1} \quad (\text{B3})$$

for  $l = x, y$  while using Eq. (12) we obtain

$$\langle j_z^{(1)} j_z^{(2)} \rangle = -\frac{1}{4(N-1)}. \quad (\text{B4})$$

Using Eq. (15), we write the correlations between collective angular momentum component of the two halves with the two-body correlations as

$$\langle J_l^a J_l^b \rangle = 4j_a j_b \langle j_l^{(1)} j_l^{(2)} \rangle = \left( \frac{N^2}{4} - \delta^2 \right) \langle j_l^{(1)} j_l^{(2)} \rangle \quad (\text{B5})$$

for  $l = x, y, z$ . Hence, using Eqs. (B3) and (B4), we obtain for the correlations between the left and right halves

$$\langle J_x^a J_x^b \rangle = \langle J_y^a J_y^b \rangle = \left( \frac{N^2}{32} - \frac{\delta^2}{8} \right) \frac{N}{N-1}, \quad (\text{B6a})$$

$$\langle J_z^a J_z^b \rangle = -\left( \frac{N}{16} - \frac{\delta^2}{4N} \right) \frac{N}{N-1}. \quad (\text{B6b})$$

Note that if we measure  $J_x$  or  $J_y$  on both sides, the measurement results will be *correlated* with each other. If we measure  $J_z$  both sides, the measurement results will be *anticorrelated* with each other.

It is worth to calculate the maximum of the correlations for any state. We obtain

$$|\langle J_l^a J_l^b \rangle| \leq j_a j_b = \frac{N^2}{16} - \frac{\delta^2}{4}, \quad (\text{B7})$$

where the bound is sharp. Note that for large  $N$  the correlations given in Eq. (B6a) are only twice less than the absolute maximum given in Eq. (B7) for  $\delta = 0$ . Thus, the Dicke state has strong correlations both in the  $x$  and  $y$  directions.

Using Eqs. (21) and (B6a), we obtain

$$\begin{aligned} [\Delta(J_l^a - J_l^b)]^2 &= [\Delta(J_l^a + J_l^b)]^2 - 4\langle J_l^a J_l^b \rangle \\ &\quad + 4\langle J_l^a \rangle \langle J_l^b \rangle \\ &= \frac{N}{8} \frac{N-2}{N-1} + \frac{1}{2} \frac{N}{N-1} \delta^2 \\ &\approx \frac{N}{8} + \frac{1}{2} \delta^2. \end{aligned} \quad (\text{B8})$$

From this, Eq. (22) follows.

### Appendix C: Quantities after experimental splitting

In this Appendix, we calculate various quantities based on the experimental splitting characterized by Eq. (29).

In order to proceed, we need that

$$\langle (J_l^s)^2 \rangle = \left( \sum_{n=1}^{N_a} j_l^{(n)} \right)^2 = \frac{j_n}{2} + 2j_n(2j_n - 1) \langle j_l^{(1)} j_l^{(2)} \rangle, \quad (\text{C1})$$

for  $s = a, b$  and  $l = x, y, z$ , where we used that  $(j_l^{(n)})^2 = \mathbb{1}/4$ . The two-point correlations are given in Eqs. (B3) and (B4). Hence, based on Eq. (17) we obtain

$$\begin{aligned} \langle (J_l^a)^2 \rangle &= \frac{N}{8} + \frac{\delta}{4} + \left( \frac{N}{2} + \delta \right) \left( \frac{N}{2} + \delta - 1 \right) \langle j_l^{(1)} j_l^{(2)} \rangle, \\ \langle (J_l^b)^2 \rangle &= \frac{N}{8} - \frac{\delta}{4} + \left( \frac{N}{2} - \delta \right) \left( \frac{N}{2} - \delta - 1 \right) \langle j_l^{(1)} j_l^{(2)} \rangle, \end{aligned} \quad (\text{C2})$$

for  $l = x, y, z$ . Now, considering Eq. (29) we arrive at Eq. (31). Based on Eq. (B6), the correlations are obtained as in Eq. (32).

### Appendix D: Derivation of the formula for the variance using normalized quantities, given in Eq. (35)

In this Appendix, we calculate various quantities for the Dicke state given in Eq. (1), in order to derive Eq. (35).

Based on Eq. (C1), the normalized second moments are obtained as

$$\begin{aligned} \frac{\langle (J_l^s)^2 \rangle}{j_n(j_n + 1)} &= \frac{1}{2(j_n + 1)} + 4 \frac{j_n - \frac{1}{2}}{j_n + 1} \langle j_l^{(1)} j_l^{(2)} \rangle \\ &\approx \frac{1}{2(j_n + 1)} + 4 \langle j_l^{(1)} j_l^{(2)} \rangle. \end{aligned} \quad (\text{D1})$$

for  $s = a, b$ , and  $l = x, y, z$ . The two-point correlations are given in Eqs. (B3) and (B4).

Let us define the difference between the normalized collective angular momentum components of the two subsystems as in Eq. (34). For the variance of  $\mathcal{J}_l^-$  we obtain

$$\begin{aligned} (\Delta \mathcal{J}_l^-)^2 &= \langle (\mathcal{J}_l^-)^2 \rangle \\ &= \frac{1}{j_a(j_a + 1)} \langle (J_l^a)^2 \rangle + \frac{1}{j_b(j_b + 1)} \langle (J_l^b)^2 \rangle \\ &\quad - 8 \sqrt{\frac{j_a j_b}{(j_a + 1)(j_b + 1)}} \langle j_l^{(1)} j_l^{(2)} \rangle \\ &\approx \frac{1}{4(j_a + 1)} + \frac{1}{4(j_b + 1)}, \end{aligned} \quad (\text{D2})$$

which leads to Eq. (35). Here, in the first equality we used Eq. (20). For the second equality we used Eq. (B5) giving the correlations. For the third, approximate equality we used the two-body correlations given in Eq. (B3) and the normalized second moments given in Eq. (D1). For the derivation, we need to use  $\sqrt{1+x} \approx 1+x/2$  to eliminate the square root.

### Appendix E: Basic ideas concerning entanglement detection

In this section, we present simple criteria that detect the Dicke state given in Eq. (1) as entangled. These criteria are not yet practical, but will help us to understand the main problems of entanglement detection in such systems.

Next, we assume that the states in the two subsystems are symmetric. Ideally, we can expect this, since the Dicke state is a symmetric multipartite state. If we split it into two subsystems, the quantum state within the subsystems is also symmetric. Hence, the quantum state can be mapped into a quantum state of two large spins.

Based on Eqs. (B6) and (29), the correlation between the two halves are obtained as in Eq. (32). The values given in Eq. (32) are very close to the values given in Eq. (B6), if we consider large  $N$  and substitute  $\delta = 0$ . Thus, the fact that there is a nonzero particle number variance during the splitting does not change these correlations a lot compared to the case when the atoms are split into two perfectly equal halves.

#### 1. Criterion based on correlations

Since we have a bipartite system, it is straightforward idea to detect entanglement based on the correlations

between the two parties. For instance, for two qubits for separable states hold [62–64]

$$|\langle j_x^{(1)} j_x^{(2)} \rangle| + |\langle j_y^{(1)} j_y^{(2)} \rangle| + |\langle j_z^{(1)} j_z^{(2)} \rangle| \leq 1/4. \quad (\text{E1})$$

For two particles of spin- $j$  a similar relation can be obtained as

$$|\langle j_x^{(1)} j_x^{(2)} \rangle| + |\langle j_y^{(1)} j_y^{(2)} \rangle| + |\langle j_z^{(1)} j_z^{(2)} \rangle| \leq j^2. \quad (\text{E2})$$

Let us consider now our Dicke state split into two equal half. Since the state is in the symmetric subspace, we can map our state into a state of two particles of spin  $j_a$  and  $j_b$ . Then, the entanglement condition reads as

$$|\langle J_x^a J_x^b \rangle| + |\langle J_y^a J_y^b \rangle| + |\langle J_z^a J_z^b \rangle| \leq j_a j_b = \frac{N^2}{16} - \frac{\delta^2}{4}, \quad (\text{E3})$$

where we have used Eq. (17). Knowing that in the experiment for the variance of  $\delta$  is Eq. (29), we obtain

$$|\langle J_x^a J_x^b \rangle| + |\langle J_y^a J_y^b \rangle| + |\langle J_z^a J_z^b \rangle| \leq \frac{N(N-1)}{16}, \quad (\text{E4})$$

which has been derived in Ref. [65]. (Note that Ref. [65] presented further interesting formulas.)

Based on Eq. (B6), for the ideal Dicke state the left-hand side of Eq. (E3) is

$$\frac{N(N+1)}{16} \frac{N}{N-1} - \delta^2 \left( \frac{1}{4} + \frac{1}{4N} \right) \frac{N}{N-1}. \quad (\text{E5})$$

If we consider the splitting for which Eq. (29) holds, then for the left-hand side of Eq. (E3) we obtain

$$\frac{N(N+1)}{16}. \quad (\text{E6})$$

The value for the Dicke state given in Eq. (E6) is very close to the bound given on the right-hand side of Eq. (E4). Hence, it is difficult to use the criterion for a real experiment. In fact, both the value for Dicke states and the bound is  $N^2/16$  in leading order in  $N$ , while their difference is proportional to  $N$  in leading order in  $N$ .

## 2. Criterion based on variances

Next, we present simple criteria that use the variances of collective observables. As an introduction, let us consider a well known criterion aimed at detecting singlet states. For separable states of a bipartite system corresponding to the  $2j_a : 2j_b$  partition [66],

$$[\Delta(J_z^a + J_z^b)]^2 + [\Delta(J_x^a + J_x^b)]^2 + [\Delta(J_y^a + J_y^b)]^2 \geq \frac{N}{2}. \quad (\text{E7})$$

holds. For multiqubit singlet states, the left-hand side of Eq. (E7) is zero, hence they maximally violate the condition.

We would like to apply our relation to Dicke states. Hence, we modify the relation

$$[\Delta(J_z^a + J_z^b)]^2 + [\Delta(J_x^a - J_x^b)]^2 + [\Delta(J_y^a - J_y^b)]^2 \geq \frac{N}{2}. \quad (\text{E8})$$

The bound for separable states remain the same, however, now the Dicke state violates the entanglement criterion Eq. (E8). For Dicke states, based on Eq. (22), the left-hand side is

$$2 \times \left( \frac{N}{8} \frac{N-2}{N-1} + \frac{1}{2} \frac{N}{N-1} \delta^2 \right) \approx \frac{N}{4} + \delta^2. \quad (\text{E9})$$

For the  $\delta = 0$  case, representing equal splitting, the Dicke state is detected as entangled. However, the criterion is not very robust. If our Dicke state has ideal correlation on the  $x$  and  $y$  directions, then  $(\Delta J_z)^2$  can grow up to around  $N/4$  such that the Dicke state is still detected. Conversely, if the correlations in the  $z$  direction are perfect, then  $[\Delta(J_x^a - J_x^b)]^2 + [\Delta(J_y^a - J_y^b)]^2$  can grow up to around by a factor of 2 to  $N/2$  and the state is still detected as entangled. Thus, the criterion tolerates very few error in  $[\Delta(J_x^a - J_x^b)]^2 + [\Delta(J_y^a - J_y^b)]^2$ , only a factor of 2 compared to the perfect Dicke state.

Let us now consider splitting as it is done in experiments, for which Eq. (29) holds. Based on Eq. (30), the left-hand side of Eq. (E8) is  $N/2$  in this case. That is, the state does not even violate the criterion given in Eq. (E8).

## Appendix F: Relation to a number-phase uncertainty relation

In this section, we attempt to connect our derivation to the literature on number-phase uncertainty relation [67–74].

If the system is described by a bosonic mode then the number phase relation is written such that the phase operator is related to the annihilation operator  $a$  of the mode. Such systems are, for example, light fields, where the superposition of states with different number of photons is possible. An EPR steering criterion has been presented in such system for two modes [33].

However, in our case we have massive particles. The superposition of quantum states with different particles numbers is not possible. In other words, the particle number is conserved. This situation can be handled by mapping each spin ensemble to two bosonic modes using the Schwinger representation [74, 75]

$$\begin{aligned} J_x &= \frac{1}{2}(a_1^\dagger a_2 + a_2^\dagger a_1), \\ J_y &= \frac{i}{2}(a_2^\dagger a_1 - a_1^\dagger a_2), \\ J_z &= \frac{1}{2}(a_1^\dagger a_1 - a_2^\dagger a_2). \end{aligned} \quad (\text{F1})$$

In this case, the role of the annihilation operator  $a$  in the number-phase uncertainty relation is played by the

operator

$$J_- = J_x - iJ_y \equiv a_1 a_2^\dagger, \quad (\text{F2})$$

where  $a_k$  are the two modes corresponding to two internal states of the particles. The operator  $J_-$  describes a process in which particles move from one mode to the other, thus the total particle number does not change.

Based on these, an uncertainty relation resembling a number-phase uncertainty has been obtained between  $J_z$  and the operator [74]

$$E_{12} = J_- / \sqrt{J_+ J_-}, \quad (\text{F3})$$

where  $J_+ = J_x + iJ_y$ , which can be further rewritten as

$$E_{12} = J_- / \sqrt{J_x^2 + J_y^2 + J_z}. \quad (\text{F4})$$

Since the angular momentum operators are defined with the Schwinger representation for two bosonic modes, the description above is appropriate to describe quantum states of two-state particles with a bosonic symmetry. However, it does not describe general quantum states of  $N$  particles that are not symmetric.

We can interpret our approach as one that defines a similar operator

$$E = J_- / \sqrt{\langle J_x^2 + J_y^2 \rangle} = C + iS, \quad (\text{F5})$$

where the operators  $C$  and  $S$  are defined as

$$C = J_x / \sqrt{\langle J_x^2 + J_y^2 \rangle}, \quad S = -J_y / \sqrt{\langle J_x^2 + J_y^2 \rangle}, \quad (\text{F6})$$

which are operators roughly corresponding to cosine and sine of the phase, and appear often in the literature about number-phase uncertainty relations. Note that we assume that the quantum state is a multi-qubit state, not necessarily with a bosonic symmetry, and  $J_l$  are just the sums of the single-particle spin components as in Eq. (10). We can rewrite Eq. (2) with these operators as

$$\left[ (\Delta J_z)^2 + \frac{1}{4} \right] [(\Delta C)^2 + (\Delta S)^2] \geq \frac{1}{4}. \quad (\text{F7})$$

- 
- [1] C. Gross, Spin squeezing, entanglement and quantum metrology with bose-einstein condensates, *J. Phys. B: At. Mol. Opt. Phys.* **45**, 103001 (2012).
- [2] J. Esteve, C. Gross, A. Weller, S. Giovanazzi, and M. Oberthaler, Squeezing and entanglement in a bose-einstein condensate, *Nature (London)* **455**, 1216 (2008).
- [3] C. Gross, T. Zibold, E. Nicklas, J. Esteve, and M. K. Oberthaler, Nonlinear atom interferometer surpasses classical precision limit, *Nature (London)* **464**, 1165 (2010).
- [4] M. F. Riedel, P. Böhi, Y. Li, T. W. Hänsch, A. Sinatra, and P. Treutlein, Atom-chip-based generation of entanglement for quantum metrology, *Nature (London)* **464**, 1170 (2010).
- [5] C. F. Ockeloen, R. Schmied, M. F. Riedel, and P. Treutlein, Quantum metrology with a scanning probe atom interferometer, *Phys. Rev. Lett.* **111**, 143001 (2013).
- [6] W. Muessel, H. Strobel, D. Linnemann, D. B. Hume, and M. K. Oberthaler, Scalable spin squeezing for quantum-enhanced magnetometry with bose-einstein condensates, *Phys. Rev. Lett.* **113**, 103004 (2014).
- [7] B. Lücke, M. Scherer, J. Kruse, L. Pezzé, F. Deuretzbacher, P. Hyllus, J. Peise, W. Ertmer, J. Arlt, L. Santos, A. Smerzi, and C. Klempt, Twin matter waves for interferometry beyond the classical limit, *Science* **334**, 773 (2011).
- [8] C. Hamley, C. Gerving, T. Hoang, E. Bookjans, and M. Chapman, Spin-nematic squeezed vacuum in a quantum gas, *Nat. Phys.* **8**, 305 (2012).
- [9] I. Apellaniz, B. Lücke, J. Peise, C. Klempt, and G. Tóth, Detecting metrologically useful entanglement in the vicinity of Dicke states, *New J. Phys.* **17**, 083027 (2015).
- [10] B. Lücke, J. Peise, G. Vitagliano, J. Arlt, L. Santos, G. Tóth, and C. Klempt, Detecting multiparticle entanglement of dicke states, *Phys. Rev. Lett.* **112**, 155304 (2014).
- [11] G. Vitagliano, I. Apellaniz, M. Kleinmann, B. Lücke, C. Klempt, and G. Tóth, Entanglement and extreme spin squeezing of unpolarized states, *New J. Phys.* **19**, 013027 (2017).
- [12] Y.-Q. Zou, L.-N. Wu, Q. Liu, X.-Y. Luo, S.-F. Guo, J.-H. Cao, M. K. Tey, and L. You, Beating the classical precision limit with spin-1 dicke states of more than 10,000 atoms, *Proceedings of the National Academy of Sciences of the United States of America* **115**, 6381 (2018).
- [13] N. Killoran, M. Cramer, and M. B. Plenio, Extracting entanglement from identical particles, *Phys. Rev. Lett.* **112**, 150501 (2014).
- [14] M. Krenn, M. Huber, R. Fickler, R. Lapkiewicz, S. Ramelow, and A. Zeilinger, Generation and confirmation of a  $(100 \times 100)$ -dimensional entangled quantum system, *Proceedings of the National Academy of Sciences* **111**, 6243 (2014).
- [15] P. Erker, M. Krenn, and M. Huber, Quantifying high dimensional entanglement with two mutually unbiased bases, *Quantum* **1**, 22 (2017).
- [16] K. Lange, J. Peise, B. Lücke, I. Kruse, G. Vitagliano, I. Apellaniz, M. Kleinmann, G. Tóth, and C. Klempt, Entanglement between two spatially separated atomic modes, *Science* **360**, 416 (2018).
- [17] A. Einstein, B. Podolsky, and N. Rosen, Can quantum-mechanical description of physical reality be considered complete?, *Phys. Rev.* **47**, 777 (1935).
- [18] M. D. Reid, Demonstration of the Einstein-Podolsky-Rosen paradox using nondegenerate parametric amplification, *Phys. Rev. A* **40**, 913 (1989).
- [19] M. D. Reid, The Einstein-Podolsky-Rosen Paradox and Entanglement 1: Signatures of EPR correlations for con-

tinuous variables, quant-ph/0112038.

- [20] M. D. Reid, P. D. Drummond, W. P. Bowen, E. G. Cavalcanti, P. K. Lam, H. A. Bachor, U. L. Andersen, and G. Leuchs, Colloquium: The Einstein-Podolsky-Rosen paradox: From concepts to applications, *Rev. Mod. Phys.* **81**, 1727 (2009).
- [21] E. G. Cavalcanti, S. J. Jones, H. M. Wiseman, and M. D. Reid, Experimental criteria for steering and the Einstein-Podolsky-Rosen paradox, *Phys. Rev. A* **80**, 032112 (2009).
- [22] Z. Y. Ou, S. F. Pereira, H. J. Kimble, and K. C. Peng, Realization of the Einstein-Podolsky-Rosen paradox for continuous variables, *Phys. Rev. Lett.* **68**, 3663 (1992).
- [23] J. Peise, I. Kruse, K. Lange, B. Lücke, L. Pezzè, J. Arlt, W. Ertmer, K. Hammerer, L. Santos, A. Smerzi, and C. Klempt, Satisfying the Einstein-Podolsky-Rosen criterion with massive particles, *Nat. Commun.* **6**, 8984 (2015).
- [24] Q. Y. He, M. D. Reid, T. G. Vaughan, C. Gross, M. Oberthaler, and P. D. Drummond, Einstein-Podolsky-Rosen entanglement strategies in two-well Bose-Einstein condensates, *Phys. Rev. Lett.* **106**, 120405 (2011).
- [25] Y. Jing, M. Fadel, V. Ivannikov, and T. Byrnes, Split spin-squeezed Bose-Einstein condensates, *New J. Phys.* **21**, 093038 (2019).
- [26] M. Fadel, T. Zibold, B. Décamps, and P. Treutlein, Spatial entanglement patterns and Einstein-Podolsky-Rosen steering in Bose-Einstein condensates, *Science* **360**, 409 (2018).
- [27] P. Kunkel, M. Prüfer, H. Strobel, D. Linnemann, A. Frölian, T. Gasenzer, M. Gärtner, and M. K. Oberthaler, Spatially distributed multipartite entanglement enables EPR steering of atomic clouds, *Science* **360**, 413 (2018).
- [28] J. K. Stockton, J. M. Geremia, A. C. Doherty, and H. Mabuchi, Characterizing the entanglement of symmetric many-particle spin- $\frac{1}{2}$  systems, *Phys. Rev. A* **67**, 022112 (2003).
- [29] Instead of Eqs. (5) and (6), typically they write [18–21]
- $$(\Delta_{\text{inf}} J_l^a)^2 = \langle (J_l^a + g_l J_l^b + d_l)^2 \rangle, \quad (\text{F8})$$
- where  $d_l$  is a number. We have to choose  $d_l$  such that the variance is minimal. This is the case if  $d_l = -\langle J_l^a + g_l J_l^b \rangle$ . With that choice,  $\langle (J_l^a + g_l J_l^b + d_l)^2 \rangle = [\Delta(J_l^a + g_l J_l^b)]^2$  holds, and we arrive at Eq. (5).
- [30] P. Hyllus, L. Pezzè, A. Smerzi, and G. Tóth, Entanglement and extreme spin squeezing for a fluctuating number of indistinguishable particles, *Phys. Rev. A* **86**, 012337 (2012).
- [31]  $[\Delta(J_l^a - J_l^b)]^2 = N/4$  always if a symmetric state is split in the condensate according to the experimental procedure. See M. Fadel and M. Gessner, Relating spin squeezing to multipartite entanglement criteria for particles and modes, *Phys. Rev. A* **102**, 012412 (2020).
- [32] R. F. Werner, Quantum states with einstein-podolsky-rosen correlations admitting a hidden-variable model, *Phys. Rev. A* **40**, 4277 (1989).
- [33] M. Fadel, L. Ares, A. Luis, and Q. He, Number-phase entanglement and Einstein-Podolsky-Rosen steering, (2020), arXiv:2002.08431.
- [34] E. G. Cavalcanti and M. D. Reid, Uncertainty relations for the realization of macroscopic quantum superpositions and epr paradoxes, *J. Mod. Opt.* **54**, 2373 (2007).
- [35] M. D. Reid and Q. Y. He, Quantifying the mesoscopic nature of Einstein-Podolsky-Rosen nonlocality, *Phys. Rev. Lett.* **123**, 120402 (2019).
- [36] B. J. Dalton, B. M. Garraway, and M. D. Reid, Tests for Einstein-Podolsky-Rosen steering in two-mode systems of identical massive bosons, *Phys. Rev. A* **101**, 012117 (2020).
- [37] V. Giovannetti, S. Mancini, D. Vitali, and P. Tombesi, Characterizing the entanglement of bipartite quantum systems, *Phys. Rev. A* **67**, 022320 (2003).
- [38] M. Kitagawa and M. Ueda, Squeezed spin states, *Phys. Rev. A* **47**, 5138 (1993).
- [39] D. J. Wineland, J. J. Bollinger, W. M. Itano, and D. J. Heinzen, Squeezed atomic states and projection noise in spectroscopy, *Phys. Rev. A* **50**, 67 (1994).
- [40] A. S. Sørensen and K. Mølmer, Entanglement and extreme spin squeezing, *Phys. Rev. Lett.* **86**, 4431 (2001).
- [41] W. Wasilewski, K. Jensen, H. Krauter, J. J. Renema, M. V. Balabas, and E. S. Polzik, Quantum noise limited and entanglement-assisted magnetometry, *Phys. Rev. Lett.* **104**, 133601 (2010).
- [42] J. Hald, J. L. Sørensen, C. Schori, and E. S. Polzik, Spin squeezed atoms: A macroscopic entangled ensemble created by light, *Phys. Rev. Lett.* **83**, 1319 (1999).
- [43] B. Julsgaard, A. Kozhekin, and E. S. Polzik, Experimental long-lived entanglement of two macroscopic objects, *Nature (London)* **413**, 400 (2001).
- [44] K. Hammerer, A. S. Sørensen, and E. S. Polzik, Quantum interface between light and atomic ensembles, *Rev. Mod. Phys.* **82**, 1041 (2010).
- [45] J. Tura, R. Augusiak, A. Sainz, B. Lücke, C. Klempt, M. Lewenstein, and A. Acín, Nonlocality in many-body quantum systems detected with two-body correlators, *Annals of Physics* **362**, 370 (2015).
- [46] R. Schmied, J.-D. Bancal, B. Allard, M. Fadel, V. Scarani, P. Treutlein, and N. Sangouard, Bell correlations in a bose-einstein condensate, *Science* **352**, 441 (2016).
- [47] S. Wagner, R. Schmied, M. Fadel, P. Treutlein, N. Sangouard, and J.-D. Bancal, Bell correlations in a many-body system with finite statistics, *Phys. Rev. Lett.* **119**, 170403 (2017).
- [48] F. Baccari, J. Tura, M. Fadel, A. Aloy, J.-D. Bancal, N. Sangouard, M. Lewenstein, A. Acín, and R. Augusiak, Bell correlation depth in many-body systems, *Phys. Rev. A* **100**, 022121 (2019).
- [49] N. Kiesel, C. Schmid, G. Tóth, E. Solano, and H. Weinfurter, Experimental observation of four-photon entangled dicke state with high fidelity, *Phys. Rev. Lett.* **98**, 063604 (2007).
- [50] W. Wieczorek, R. Krischek, N. Kiesel, P. Michelberger, G. Tóth, and H. Weinfurter, Experimental entanglement of a six-photon symmetric dicke state, *Phys. Rev. Lett.* **103**, 020504 (2009).
- [51] R. Prevedel, G. Cronenberg, M. S. Tame, M. Paternostro, P. Walther, M. S. Kim, and A. Zeilinger, Experimental realization of dicke states of up to six qubits for multiparty quantum networking, *Phys. Rev. Lett.* **103**, 020503 (2009).
- [52] G. Tóth, Detection of multipartite entanglement in the vicinity of symmetric Dicke states, *J. Opt. Soc. Am. B* **24**, 275 (2007).
- [53] D. M. Greenberger, M. A. Horne, A. Shimony, and



- A. Zeilinger, Bell's theorem without inequalities, *Am. J. Phys.* **58**, 1131 (1990).
- [54] D. Bouwmeester, J.-W. Pan, M. Daniell, H. Weinfurter, and A. Zeilinger, Observation of three-photon Greenberger-Horne-Zeilinger entanglement, *Phys. Rev. Lett.* **82**, 1345 (1999).
- [55] J.-W. Pan, D. Bouwmeester, M. Daniell, H. Weinfurter, and A. Zeilinger, Experimental test of quantum nonlocality in three-photon Greenberger-Horne-Zeilinger entanglement, *Nature (London)* **403**, 515 (2000).
- [56] Z. Zhao, T. Yang, Y.-A. Chen, A.-N. Zhang, M. Żukowski, and J.-W. Pan, Experimental violation of local realism by four-photon Greenberger-Horne-Zeilinger entanglement, *Phys. Rev. Lett.* **91**, 180401 (2003).
- [57] C.-Y. Lu, X.-Q. Zhou, O. Gühne, W.-B. Gao, J. Zhang, Z.-S. Yuan, A. Goebel, T. Yang, and J.-W. Pan, Experimental entanglement of six photons in graph states, *Nat. Phys.* **3**, 91 (2007).
- [58] W.-B. Gao, C.-Y. Lu, X.-C. Yao, P. Xu, O. Gühne, A. Goebel, Y.-A. Chen, C.-Z. Peng, Z.-B. Chen, and J.-W. Pan, Experimental demonstration of a hyper-entangled ten-qubit schrödinger cat state, *Nat. Phys.* **6**, 331 (2010).
- [59] D. Leibfried, M. Barrett, T. Schaetz, J. Britton, J. Chiaverini, W. Itano, J. Jost, C. Langer, and D. Wineland, Toward heisenberg-limited spectroscopy with multiparticle entangled states, *Science* **304**, 1476 (2004).
- [60] C. Sackett, D. Kielpinski, B. King, C. Langer, V. Meyer, C. Myatt, M. Rowe, Q. Turchette, W. Itano, D. Wineland, and C. Monroe, Experimental entanglement of four particles, *Nature (London)* **404**, 256 (2000).
- [61] T. Monz, P. Schindler, J. T. Barreiro, M. Chwalla, D. Nigg, W. A. Coish, M. Harlander, W. Hänsel, M. Hennrich, and R. Blatt, 14-qubit entanglement: Creation and coherence, *Phys. Rev. Lett.* **106**, 130506 (2011).
- [62] G. Tóth, Entanglement witnesses in spin models, *Phys. Rev. A* **71**, 010301 (2005).
- [63] C. Brukner and V. Vedral, Macroscopic Thermodynamical Witnesses of Quantum Entanglement, eprint arXiv:quant-ph/0406040 (2004).
- [64] M. R. Dowling, A. C. Doherty, and S. D. Bartlett, Energy as an entanglement witness for quantum many-body systems, *Phys. Rev. A* **70**, 062113 (2004).
- [65] E. Oudot, J.-D. Bancal, R. Schmied, P. Treutlein, and N. Sangouard, Optimal entanglement witnesses in a split spin-squeezed Bose-Einstein condensate, *Phys. Rev. A* **95**, 052347 (2017).
- [66] G. Tóth, Entanglement detection in optical lattices of bosonic atoms with collective measurements, *Phys. Rev. A* **69**, 052327 (2004).
- [67] P. Carruthers and M. M. Nieto, Phase and angle variables in quantum mechanics, *Rev. Mod. Phys.* **40**, 411 (1968).
- [68] R. Lynch, The quantum phase problem: a critical review, *Phys. Rep.* **256**, 367 (1995).
- [69] J.-M. Lévy-Leblond, Who is afraid of nonhermitian operators? A quantum description of angle and phase, *Ann. Phys.* **101**, 319 (1976).
- [70] D. T. Pegg and S. M. Barnett, Unitary phase operator in quantum mechanics, *Europhys. Lett.* **6**, 483 (1988).
- [71] S. Barnett and D. Pegg, On the Hermitian optical phase operator, *J. Mod. Opt.* **36**, 7 (1989).
- [72] D. T. Pegg and S. M. Barnett, Phase properties of the quantized single-mode electromagnetic field, *Phys. Rev. A* **39**, 1665 (1989).
- [73] J. Vaccaro and D. Pegg, Physical number-phase intelligent and minimum-uncertainty states of light, *J. Mod. Opt.* **37**, 17 (1990).
- [74] A. Luis and L. L. Sánchez-Soto, Phase-difference operator, *Phys. Rev. A* **48**, 4702 (1993).
- [75] I. Urizar-Lanz and G. Tóth, Number-operator-annihilation-operator uncertainty as an alternative for the number-phase uncertainty relation, *Phys. Rev. A* **81**, 052108 (2010).